A study of white etching crack formation by compression-torsion experiments

S. Averbeck, E. Kerscher

Materials Testing (AWP), University of Kaiserslautern, Gottlieb-Daimler-Strasse, 67663 Kaiserslautern, Germany
stefan.averbeck@mv.uni-kl.de, kerscher@mv.uni-kl.de

ABSTRACT. In this study, an attempt was made to recreate the bearing damage phenomenon "White Etching Cracks" with a simplified testing setup. Rolling contact fatigue conditions were simulated with in-phase and out-of-phase cyclic compression-torsion experiments on 100Cr6 steel specimens. The results are compared in terms of microstructural change. Focused Ion Beam and metallographic analysis reveal that a fine-grained, white etching zone formed in the vicinity of the fatigue cracks of specimens tested with the in-phase load pattern. In contrast, no such structures were found after testing the out-of-phase load pattern. The properties of the white etching zone are characterised in more detail and compared with White Etching Cracks.

KEYWORDS. White Etching Cracks; Multiaxial fatigue; Bearing steel.

INTRODUCTION

In the past two decades, increasing attention has been focused on the damage mechanism "White Etching Cracks" (WEC). WECs can lead to very early bearing failure (usually 5-20% of L_{10}) under operating conditions that would usually allow the bearing to achieve its calculated service life [1]. Despite intensive research and a variety of root cause hypotheses, no comprehensive explanation for WEC formation exists yet. The phenomenon seems to be influenced by multiple parameters which are often interdependent. The different hypotheses and influencing factors have been reviewed by Gegner [2], Evans [1] and, more recently, by Stadler et al. [3].

The characteristic feature of White Etching Cracks is the appearance of the crack faces, which appear white when etched with 3% nitric acid. This etching behaviour is attributed to an extreme grain refinement compared to the original martensitic structure. The average grain size is reduced from ~1μm to 10-100nm [2, 4]. The reduction in grain size is coupled with an increase in hardness from about 700HV to 1000HV and above [1, 5], in part due to the Hall-Petch effect, in part due to the dissolution of carbides in the white etching area [4]. The lattice structure is body-centred cubic, which is carbon-supersaturated ferrite [1, 2], although amorphous structures have also been reported [6]. WEC have a tendency to branch and form networks or groups [1, 7]. This heavy branching of the cracks and their three-dimensional interconnections are responsible for their detrimental effect on bearing life, as this structure easily leads to spalling damage.

WECs are found almost exclusively near or at the surface of bearing components, although they can propagate very deeply into the material [8]. It is therefore assumed that there is a link to rolling contact fatigue (RCF) mechanisms, which

are caused by the cyclic Hertzian stresses in the contact area. This complex superposition of compressional and shear stresses changes over time as a rolling element passes over the raceway. In this area, defects, such as non-metallic inclusions or voids, can act as stress concentrators and enable crack initiation. A phenomenon called 'butterflies' which occurs in this region has been linked to White Etching Crack formation [9]. These are cracks around inclusions which are accompanied by white etching areas with virtually the same properties. It has to be considered, though, that butterflies are always oriented at 20-30 degrees to the contact surface, whereas WECs are not specifically oriented in any direction [1, 8].

EXPERIMENTS

This study differs from earlier WEC investigations in its approach to WEC reproduction. Instead of testing bearings, simple hourglass-shaped specimens made from 100Cr6 steel were used (Fig. 1). The specimens were heat treated at the SKF GmbH bearing manufacturing plant in Schweinfurt, Germany, according to the regular bearing heat treatment standards of SKF. After heat treatment, the specimens were ground to a roughness R_z of 2μm and subsequently polished.
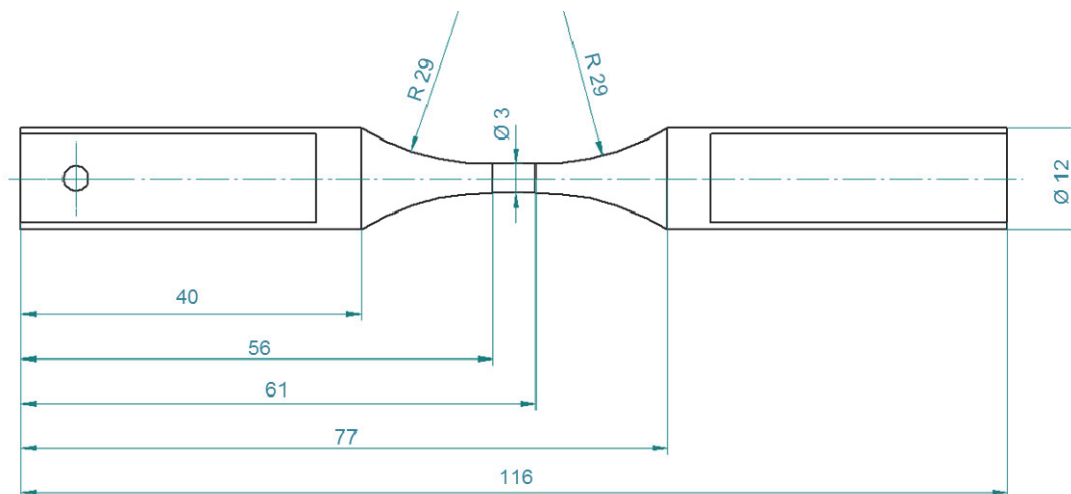

Figure 1: Specimen geometry.

Load-controlled testing was carried out with superimposed axial and torsional loads on a servohydraulic MTS 858 testing machine. Two different approaches to the reproduction of rolling contact fatigue were used: in-phase and out-of-phase loading. For both load spectra, tests were performed in air and in partially synthetic SAE 75/W80 transmission oil with a specific additive package. This is a typical gearbox oil which has been found to promote WEC formation, most likely due to its additives [10]. All experiments were carried out at room temperature.

In-phase loading

Transfer between RCF conditions and in-phase loading was based on achieving a similar highest equivalent stress. Although the stress state in a bearing constantly changes over time, it is possible to identify a time and location where the equivalent stress is highest during one load cycle. This stress state can be modelled by in-phase compressional and torsional load, as demonstrated by Burkart et al. [11]. The equivalent stresses were determined using von Mises' criterion and applied such that the ratio between the principal stresses' difference, $|\sigma_I - \sigma_{II}| / |\sigma_{II} - \sigma_{III}|$, was the same in the experiment as in a real bearing. There remains, of course, one main difference between a bearing and the experiment: while the maximum stress is located beneath the surface in the former, it occurs at the surface in the specimen.

Out-of-phase loading

This load spectrum was based on work by Beretta and Foletti [12], who used out-of-phase compression-torsion loads to study coplanar crack propagation from artificial defects. They tested bearing steel specimens with two different load patterns, which were proposed by bearing manufacturer SKF. The first pattern aimed at reproducing subsurface conditions, while the second should reproduce the conditions deeper under the bearing surface. It was found that only the

second pattern led to coplanar crack propagation, which can be interpreted as a sign that it better recreated RCF conditions. For this reason and for ease of controller programming, we adopted the second pattern, which is described below, for our study.

The load pattern is defined by a) the phase shift between the compression and torsional loads and b) the ratio between maximum torsional and maximum compressional stress. With a phase shift of 90 degrees, the specimen experiences half of the maximum compression at the time of highest torsional stress. The ratio between the maximum stresses, σ_{max}/τ_{max}, is stated to be about 3.75 in [12]. With the proportion of the stresses thus set, the question remains which absolute values of stress are to be used. The equivalent stress can be made to match bearing conditions either at the time of maximum torsional stress, or at maximum compressional stress. Both variants can be justified: the former causes the same stress state at the equivalent stress that is relevant for a bearing, but causes much greater equivalent stresses between the torsional maxima. The other variant, meanwhile, ensures that both the in-phase and the out-of-phase specimens are subjected to the same maximum equivalent stress but leads to a different stress state at the torsional maxima with lower equivalent stress. Both variants were tested during our experiments, designated OOP-A and OOP-B.

As WECs mostly lead to bearing failures in the early high cycle fatigue range, it was decided to run the fatigue tests only up to 10^6 cycles. This means that even with a limited load frequency of 10Hz, it was possible to use realistic stress levels. As none of the in-phase and OOP-B specimens fractured during testing, they were fatigued until fracture under alternating torsion with superimposed constant tension.

All specimens were cleaned in acetone and ethanol in an ultrasonic bath before the microstructural examinations. Afterwards, all specimens were examined with the scanning electron microscope. Select specimens were studied in more detail with the combined SEM/Focused Ion Beam (FIB) at the Nanostructuring Center (NSC) of the University of Kaiserslautern. Furthermore, some specimens were hot mounted in epoxy resin and subsequently ground, polished, and etched with 3% nitric acid (nital) for metallographic investigations. Finally, microhardness tests were carried out using a diamond Berkovich indenter at 50mN load.
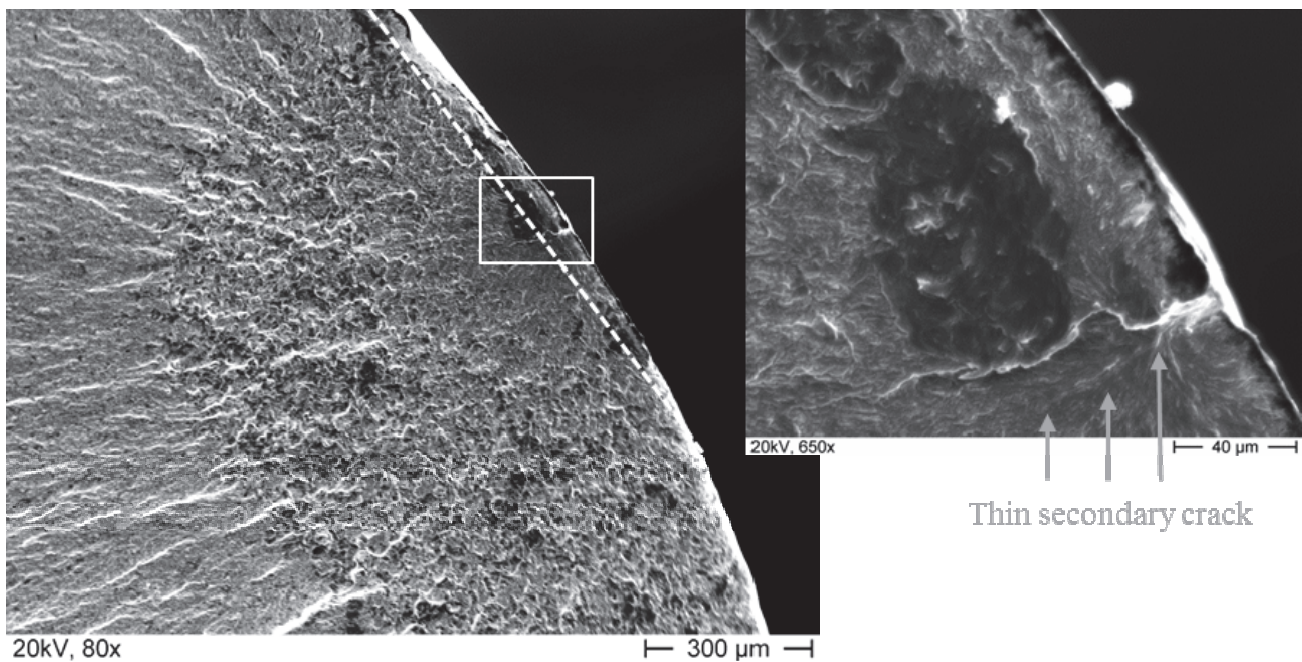

Figure 2: Fracture surface of an in-phase specimen tested in air. The approximate position of the metallographic section in Fig. 4 is indicated by the dashed line.

RESULTS

In-phase experiments

Fig. 2 shows the fracture surface around the crack starting point after in-phase testing. The image is representative for specimens tested in air and in oil alike. There are three distinct regions with different fracture morphologies: a small lens at the specimen's surface indicating the crack propagation during in-phase loading, a second area showing the fracture surface of stable crack growth during fatigue loading to fracture the specimen, and a third area of

final fracture. At higher magnification, a step can be seen between the upper and the lower half of the lens. This indicates that the crack propagated orthogonally to the specimen axis until it reached a length of 5-10µm, at which point the further crack propagation was controlled by mode I, i.e. perpendicular to the highest shear stress.

It is possible that this change of direction coincides with the change from compression-torsion testing to torsional fracturing; however, it is equally possible that the crack propagation mode changed already during the testing phase, as fatigue cracks often change direction during their growth under multiaxial load conditions [13]. Considering the morphological differences within the fatigue lens – a relatively smooth innermost area followed by a much coarser structure more outwardly – makes the latter explanation seem more likely, as this suggests a change of the crack growth mechanism. If this interpretation is correct, the fatigue crack propagated around 250µm during in-phase loading. A grainy surface structure can be observed at small scales near the above-mentioned step, and a very thin secondary crack extends from the surface to a depth of about 50µm.

In order to examine the microstructure below the surface, Focused Ion Beam (FIB) cuts with a length of 30µm were made at two points on the fracture surface. This allowed for studying the top 5µm of the specimen microstructure. In both cut areas, a very fine-grained layer with a thickness of no more than 500nm could be observed at the surface (Fig. 3). This grain refinement was not affected by whether the test was run in oil or air. A carbide is observable in the transition zone between the nanocrystalline structure and the unaltered material below. It could be argued that its shape indicates deformation and the onset of dissolution; this, however, remains debatable.
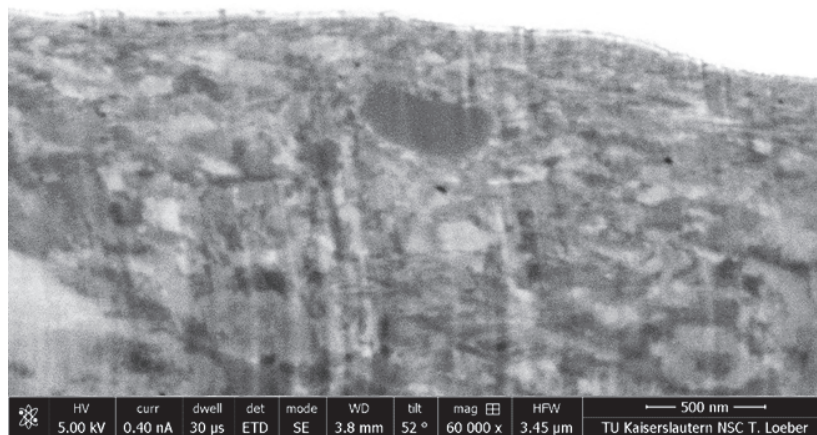

Figure 3: SEM image of grain refinement and a carbide in the surface layer.
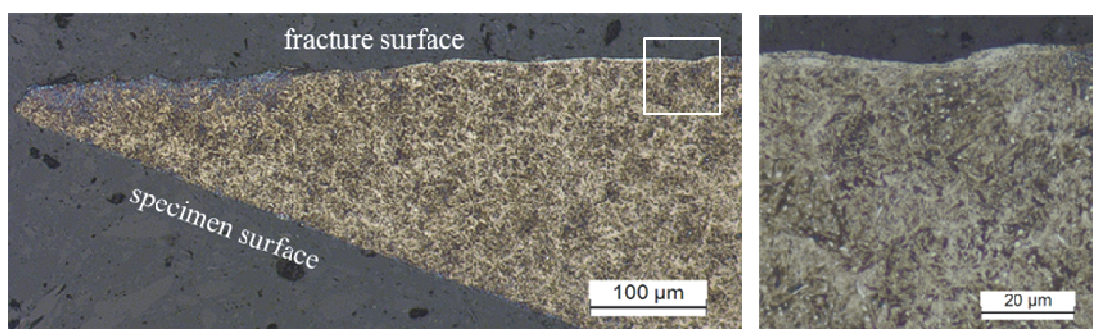

Figure 4: Metallographic section of an in-phase specimen tested in air. The smaller image on the right is a magnification of the marked area.

A metallographic examination of the opposite fracture surface reveals a white-etching zone on the fracture surface (Fig. 4). Under the light optical microscope (LOM), this zone appears largely featureless with interspersed carbides. The thickness of the zone is around 1µm. Its lateral dimension is much greater, spanning several hundred micrometres. This matches the diameter of the inner fatigue lens in Fig. 2. The white etching zone remained visible after further grinding, polishing, and etching with about 50µm material removal.

Microhardness measurements in the white etching zone varied from 753HV to 1246HV, with an average value of 986HV (five measurements). This is significantly harder than the original martensitic microstructure, which has a hardness of 700-750HV.

Out-of-phase experiments

In contrast, no microstructurally changed areas could be found after the out-of-phase tests, independently of the surrounding medium (oil or air). The OOP-A cycle was only used for very few tests, as it became apparent that specimens fractured very early in the high cycle fatigue regime or even in the low cycle fatigue regime ($N_B < 10^5$).

The OOP-B tests showed no signs of microstructural change, although the cracks propagated in the same manner like the in-phase fatigue cracks. In some specimens, no crack formation was observed at all during the 10^6 cycles of testing.

DISCUSSION

White etching microstructural changes are not an exclusive feature of White Etching Cracks, as the white layers found on rail steel (e.g. [14]) or in dry sliding contacts (e.g. [15]) demonstrate. It is thus necessary to carefully examine whether the zone formed during the compression-torsion experiments really is similar to WEC microstructural change, and to eliminate any other formation possibilities and error sources. For example, the fracture stage which followed the testing cycle could have caused the microstructural changes. However, when comparing the in-phase results with those of the OOP-B tests, this becomes very unlikely. If the white etching layer was formed due to the torsional fracturing stage, it should appear on all specimens, not only on those tested in-phase.

Many formation mechanisms for white etching microstructure rely on a thermal component. This is especially true for the examples in dry sliding contacts mentioned above. No signs for thermal influences have been found in the experimental results. The fact that the white layers formed regardless of whether the specimen was tested in air or in oil rules out a mechanism like those in dry sliding contacts.

Aside from these aspects *ex negativo*, the white etching surface layer produced by in-phase testing is in several aspects similar to the altered microstructure found in WECs. The FIB images, for example, closely resemble those presented by Franke et al. [16]. When viewed in the light optical microscope, the appearance of the white etching structure is very similar to WEC found in the literature. The hardness values also closely match those reported for WEC. The thickness of the white etching structures never exceeded 1μm in the specimen, mostly amounting to only a few hundred nanometres. This is well within the range reported for bearing WECs; however, the volume of white etching microstructure can vary widely in bearings [8].

In most cases, the cracks did not seem to develop branches. Small cracks at an angle to the fracture surface could be found in some specimens, one example being shown in Fig. 2. Whether this is a genuine WEC-type branch or simply a secondary crack from fatigue and fracture presently cannot be answered. An additional FIB cut might serve to clarify this. The cracks never seemed to nucleate at inclusions or voids; at least, no traces of such were found in the vicinity. It is therefore assumed that either surface or microstructural inhomogeneities were responsible for crack initiation.

The most ambiguous aspect of the results is the question of carbides. While they are usually absent or in the process of dissolution in bearing WECs, their presence is no decisive argument against WECs [6]. Judging from the light optical microscope observations, numerous carbides were interspersed in the white etching areas found in this study. The limited magnification of the LOM makes it impossible to assess whether they are affected by the surrounding microstructural change. Nor could the FIB investigation deliver a conclusive result. While the carbide in Fig. 3 might be dissolving, others retained a largely globular shape with sharp borders to the surroundings. Generally, it should be remembered that the testing time of 10^6 cycles was moderate. A longer test, e.g. up to 10^7 cycles, could serve to clarify whether carbides dissolve or not. This could also provide insights to whether the thickness of the white structure will further increase over time or not.

The early failures under load spectrum OOP-A were probably a result not only of the higher equivalent stresses, but also of the 90° phase shift. Fatemi and Shamsaei [13] cite several reports that out-of-phase loads have a significantly more detrimental effect on fatigue properties than in-phase loads. The higher compressional loads themselves probably would not be as problematic, as they would tend to close any incipient cracks.

No satisfactory explanation could be found for the behaviour of the OOP-B tests, in which no observable microstructural change was found despite the fact that the crack paths were very similar to those from in-phase testing. The most obvious explanation is that the equivalent stresses were too low in the crucial points in each cycle, i.e. at the time of maximum

torsional loading. It is also possible that the ratio between compressional and torsional load at the torsional maxima prevented microstructural change and even crack formation, as was the case in several specimens.

SUMMARY

Rolling contact fatigue conditions were simulated with in-phase and out-of-phase cyclic multiaxial loads. It was found that the material behaviour differed greatly between the two load patterns. While the out-of-phase load led to regular crack initiation and propagation, zones of altered microstructure were found adjacent to fatigue cracks in the in-phase specimens. Detailed investigations with SEM, FIB, nanoindentation and metallographic methods revealed that these zones resemble the microstructural change in the bearing damage phenomenon White Etching Cracks.

ACKNOWLEDGEMENTS

REFERENCES

[1] Evans, M.-H., White structure flaking (WSF) in wind turbine gearbox bearings: effects of 'butterflies' and white etching cracks (WECs), Tribol. Int., 28 (2012) 3–22.

[2] Gegner, J., Tribological Aspects of Rolling Bearing Failures, in: Kuo, C.-H. (Ed.), Tribology - Lubricants and Lubrication, InTech, Rijeka, (2011) 33–93.

[3] Stadler, K., Lai, J., Vegter, R.H., A Review: The Dilemma With Premature White Etching Crack (WEC) Bearing Failures, in: Beswick, J.M. (Ed.), Bearing Steel Technologies, ASTM International, West Conshohocken, (2014) 487–508.

[4] West, O., Diederichs, A.M., Alimadadi, H., Dahl, K.V., Somers, M., Application of Complementary Techniques for Advanced Characterization of White Etching Cracks, Pract. Metallogr., 50 (2013) 410–431.

[5] Greco, A., Sheng, S., Keller, J., Erdemir, A., Material wear and fatigue in wind turbine Systems, Wear, 302, (2012) 1583–1591.

[6] Harada, H., Mikami, T., Shibata, M., Sokai, D., Yamamoto, A., Tsubakino, H., Microstructural Changes and Crack Initiation with White Etching Area Formation under Rolling/Sliding Contact in Bearing Steel, ISIJ Int., 45 (2005) 1897–1902.

[7] Evans, M.-H., Wang, L., Jones, H., Wood, R., White etching crack (WEC) investigation by serial sectioning, focused ion beam and 3-D crack modelling, Tribol. Int., 65 (2013) 146–160.

[8] Ruellan Du Crehu, Arnaud, Tribological analysis of White Etching Crack (WEC) failures in Rolling Element Bearings, PhD thesis, INSA Lyon, (2014).

[9] Evans, M.-H., Richardson, A.D., Wang, L., Wood, R.J.K., Anderson, W.B., Confirming subsurface initiation at non-metallic inclusions as one mechanism for white etching crack (WEC) formation, Tribol. Int., 75 (2014) 87–97.

[10] Surborg, H., Einfluss von Grundölen und Additiven auf die Bildung von WEC in Wälzlagern, Shaker, Aachen, (2014).

[11] Burkart, K., Bomas, H., Schroeder, R., Zoch, H.-W., Rolling Contact and Compression-Torsion Fatigue of 52100 Steel with Special Regard to Carbide Distribution, in: Beswick, J.M. (Ed.), Bearing Steel Technologies, ASTM International, West Conshohocken, (2012) 218–236.

[12] Beretta, S., Foletti, S., Propagation of small cracks under RCF: a challenge to Multiaxial Fatigue Criteria, in: Carpinteri, A., Iacoviello, F., Pook, L.P., Susmel, L. (Eds.), Proceedings of the 4th International Conference on Crack Paths (CP 2012), Gruppo Italiano Frattura, Cassino, (2012) 15–28.

[13] Fatemi, A., Shamsaei, N., Multiaxial fatigue: An overview and some approximation models for life estimation, Int. J. Fatigue, 33 (2011) 948–958.

[14] Baumann, G., Fecht, H.J., Liebelt, S., Formation of white-etching layers on rail treads, Wear, 191, (1996) 133–140.

[15] Griffiths, B.J., Mechanisms of White Layer Generation With Reference to Machining and Deformation Processes, J. Tribol., 109 (1987) 525–530.

[16] Franke, J., Surborg, H., Fahl, J., Elfrath, T., Blass, T., Holweger, W., Merk, D., Influence of Tribolayer on WEC Roller Bearing Fatigue Performed on a FE8 Test Rig, in: Proceedings TAE - 19th International Colloquium Tribology, Technische Akademie Esslingen, Esslingen, (2014) 163–175.